Assembly factors for the membrane arm of human complex I

Byron Andrews, Joe Carroll, Shujing Ding, Ian M. Fearnley, and John E. Walker[1]

Medical Research Council Mitochondrial Biology Unit, Cambridge CB2 0XY, United Kingdom

Contributed by John E. Walker, October 14, 2013 (sent for review September 12, 2013)

Mitochondrial respiratory complex I is a product of both the nuclear and mitochondrial genomes. The integration of seven subunits encoded in mitochondrial DNA into the inner membrane, their association with 14 nuclear-encoded membrane subunits, the construction of the extrinsic arm from 23 additional nuclear-encoded proteins, iron–sulfur clusters, and flavin mononucleotide cofactor require the participation of assembly factors. Some are intrinsic to the complex, whereas others participate transiently. The suppression of the expression of the NDUFA11 subunit of complex I disrupted the assembly of the complex, and subcomplexes with masses of 550 and 815 kDa accumulated. Eight of the known extrinsic assembly factors plus a hydrophobic protein, C3orf1, were associated with the subcomplexes. The characteristics of C3orf1, of another assembly factor, TMEM126B, and of NDUFA11 suggest that they all participate in constructing the membrane arm of complex I.

mitochondria | respiratory chain | NADH:ubiquinone oxidoreductase

In mammalian mitochondria, complex I (NADH:ubiquinone oxidoreductase) provides the entry point for electrons from NADH into the electron transport chain. For each two electrons transferred from NADH to ubiquinone, four protons are ejected from the mitochondrial matrix, thereby contributing to the proton motive force across the inner membrane (1). The mammalian enzyme has 44 subunits, with a combined molecular mass of about 1 MDa, assembled into an L-shaped complex, with one arm embedded in the inner membrane and the other protruding into the matrix of the organelle (2–4). Seven hydrophobic subunits (ND1–ND6 and ND4L) of the membrane arm of NADH dehydrogenase (complex I) are encoded in mitochondrial DNA, and synthesized on mitochondrial ribosomes (5). The remainder are nuclear gene products, made in the cytoplasm and imported into mitochondria (6). The seven proteins encoded in mitochondrial DNA and seven nuclear-encoded subunits conserved in prokaryotic complexes I, constitute the catalytic cores of the membrane and peripheral arms, respectively (1). The latter contains binding sites for NADH, the primary electron acceptor FMN, and seven iron–sulfur clusters that link FMN and the terminal electron acceptor, ubiquinone, bound at the juncture between the peripheral and membrane arms (1, 7). The membrane arm has four antiporter-like domains that probably provide pathways for translocating protons (1). The remaining 30 so-called supernumerary subunits of mammalian complex I have no direct role in catalysis (2). Their functions are mostly unknown, but they may be involved in assembly, stability, or regulation of the complex (2, 8).

There is no atomic structure for any eukaryotic complex I, but the arrangement and folds of the 14 core subunits in the mammalian enzyme are likely to be closely similar to those of bacterial orthologs, with the supernumerary subunits attached peripherally around the core (2, 9). The distribution of supernumerary subunits in bovine complex I is known from the subunit compositions of subcomplexes (3, 10, 11). Subcomplex Iλ is the peripheral arm, subcomplex Iα is a combination of Iλ and the adjacent region of the membrane arm, subcomplex Iβ is the distal region of the membrane arm, and subcomplex Iγ is another fragment from the membrane arm. The supernumerary subunits in a fungal enzyme from *Yarrowia lipolytica* seem to be distributed similarly (12, 13).

The assembly of mitochondrial complex I involves building the 44 subunits emanating from two genomes into the two domains of the complex. The enzyme is put together from preassembled subcomplexes, and their subunit compositions have been characterized partially (14, 15). Extrinsic assembly factors of unknown function become associated with subcomplexes that accumulate when assembly and the activity of complex I are impaired by pathogenic mutations. Some assembly factor mutations also impair its activity (16). Other pathogenic mutations are found in all of the core subunits, and in 10 supernumerary subunits (NDUFA1, NDUFA2, NDUFA9, NDUFA10, NDUFA11, NDUFA12, NDUFB3, NDUFB9, NDUFS4, and NDUFS6) (17–26). Those in supernumerary subunits NDUFA2, NDUFA10, NDUFS4, and NDUFS6 are associated with a reduced level of intact complex and accumulation of subcomplexes, indicating a defect in assembly or stability of the complex, or both.

As described here, suppression of the expression of the supernumerary membrane subunit NDUFA11 impairs assembly of complex I, leading to the accumulation of subcomplexes with estimated molecular masses of 550 and 815 kDa associated with eight known assembly factors, plus three other proteins, especially C3orf1. NDUFA11 has the characteristics of an intrinsic assembly factor for complex I and together with C3orf1 and another extrinsic assembly factor TMEM126B (27), they probably help to assemble the membrane arm of the complex.

Results

Suppression of Expression of NDUFA11. The experiment, conducted in 143B cells, had three effects. First, cellular oxygen consumption linked to complex I was reduced by two-thirds (Fig. 1), and

Significance

Mammalian complex I, the largest and most complicated enzyme of the mitochondrial respiratory chain, is an L-shaped assembly of 44 proteins with one arm in the mitochondrial matrix and the orthogonal arm buried in the inner membrane. It is put together from preassembled modules. This investigation concerns the little studied process of the assembly of the membrane arm module from proteins emanating from both nuclear and mitochondrial genomes. We have identified two membrane protein assembly factors C3orf1 and TMEM126B, not found in the mature complex, that help this process by putting together two membrane arm subcomplexes. Defects in the assembly of complex I are increasingly being associated with human pathologies.

Author contributions: B.A. and J.E.W. designed research; B.A., J.C., S.D., and I.M.F. performed research; B.A., J.C., S.D., I.M.F., and J.E.W. analyzed data; and J.E.W. wrote the paper.

The authors declare no conflict of interest.

Freely available online through the PNAS open access option.

[1]To whom correspondence should be addressed. E-mail: walker@mrc-mbu.cam.ac.uk.

This article contains supporting information online at www.pnas.org/lookup/suppl/doi:10.1073/pnas.1319247110/-/DCSupplemental.

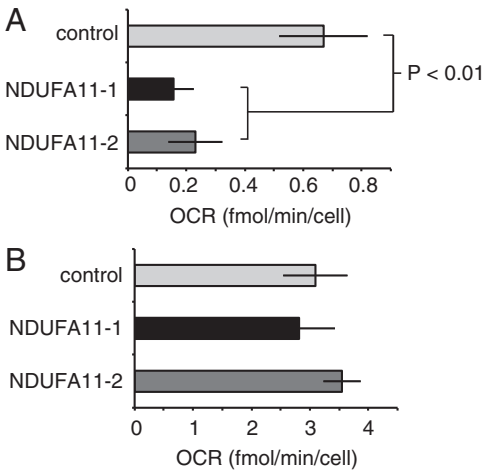

Fig. 1. Oxygen consumption of 143B cells with ablated NDUFA11. Oxygen consumption rate (OCR) 96 h after transfection with two siRNAs (NDUFA11-1 and -2, each 30 nM) against NDUFA11 (black and dark gray) compared with control cells (light gray). (*A*) Complex-I–dependent OCR of 143B cells determined by subtraction of rotenone-inhibited OCR values from initial values. (*B*) Addition of rotenone and duroquinol and OCR derived from activities of complexes III and IV. Error bars are SD.

the effect was bypassed by addition of the complex III substrate, duroquinol. Second, the mitochondrial network observed in control cells became fragmented (Fig. S1). Third, the amount of intact complex I was reduced, and subcomplexes with molecular masses of 815 and 550 kDa accumulated (Fig. 2). Previously known as the 830- and 650-kDa subcomplexes, respectively (16), their sizes have been reestimated (Fig. S2). This accumulation of the 815-kDa complex is similar to the effects of mutation of NDUFS4 or NDUFAF2 (28), but the accumulation of the 550-kDa complex has not been reported.

Association of C3orf1 and TMEM126B with Incompletely Assembled Complex I. A 143B cell line in which NDUFA11 had been suppressed stably was subjected to stable isotope labeling of amino acids in cell culture (SILAC) so as to quantify differences in protein levels relative to control cells, by mass spectrometry. As there were no significant changes in protein abundance, expression rates, or degradation (Dataset S1), any changes in the

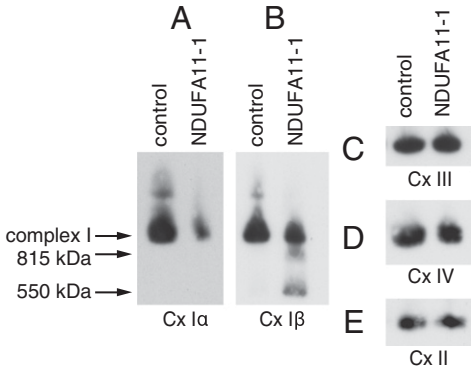

Fig. 2. Effect of transient suppression of the expression of NDUFA11 on assembly of complex I. Analysis by BN-PAGE of mitoplasts from 143B cells following suppression of expression of NDUFA11 with siRNA NDUFA11-1 for 96 h. (*A*–*E*) Protein complexes detected with antibodies against subunits of the hydrophilic arm of complex I (NDUFS1), the hydrophobic arm of complex I (NDUFB8), and complexes III, IV, and II, respectively.

protein profile of complex I accompanying the eightfold reduction of NDUFA11 correspond to additional proteins associated with incompletely assembled complex I. Eight known assembly factors, NDUFAF1–4, ACAD9, ECSIT, FOXRED1, and TMEM126B were associated with the NDUFA11-deficient subcomplexes (Fig. 3 and Dataset S1). FOXRED1 has been designated as an assembly factor from genetic and functional data (29), but here its direct association with assembly intermediates of complex I has been demonstrated. Three other proteins, C3orf1, ATP5SL, and DNAJC11 were found. C3orf1 and ATP5SL have no ascribed functions, whereas DNAJC11 belongs to the Hsp40 chaperone family. Both C3orf1 and TMEM126B colocalized with MitoTracker, and so they are intrinsic mitochondrial proteins (Fig. S3).

Ablation of C3orf1, TMEM126B, ATP5SL, and DNAJC11 and Assembly of Complex I. The suppression of expression of C3orf1 or TMEM126B reduced both the cellular oxygen consumption, and the level of intact complex I (Fig. 4), and subcomplexes of 315 and 370 kDa accumulated. They were detected with antibodies against the peripheral arm and the membrane arm component NDUFB8, respectively. The accumulation of the 370-kDa subcomplex was concomitant with a reduction in a 550-kDa subcomplex (Fig. 4), presumably the same subcomplex accompanying suppression of expression of NDUFA11 (Fig. 2). Also, when TMEM126B was suppressed, the levels of both complexes III and IV increased (Fig. 4). As the analyses were performed in the presence of n-dodecyl-β-D-maltoside, which dissociates respiratory complexes into individual enzymes, the increase in complexes III and IV is not due to their release from supercomplexes. In their experiments on TMEM126B, Heide et al. reported an increase in complex III, but not of complex IV (27).

The complex I assembly factors NDUFAF3, ACAD9, and NDUFAF2 are associated with subassemblies with masses of 400, 460, and 830 kDa, respectively (15). Based on the reestimated masses of subcomplexes (Fig. S2) they probably correspond to the 315-, 370-, and 815-kDa subcomplexes, respectively, described here. This conclusion is supported by the distributions of NDUFAF2, NDUFAF3, and ACAD9 in subcomplexes derived from cells treated with siRNAs directed against TMEM126B and NDUFA11 (Fig. S4); NDUFAF3, ACAD9, and NDUFAF2 were associated with subcomplexes with the revised masses of 315, 370, and 815 kDa, respectively.

In contrast, suppression of expression of either ATP5SL or DNAJC11, or both proteins together, had no effect on the assembly of complex I (Fig. S5).

Copurification of C3orf1 with the 315-kDa Subcomplex. Attempts were made to introduce versions of C3orf1 and TMEM126B with C-terminal StrepII and FLAG tags into HeLa Flp-In T-Rex cells, but only the expression of C3orf1 with tags (C3orf1-FL) succeeded.

The protein interactions of C3orf1 were examined by SILAC labeling of cells expressing C3orf1-FL. The mass spectrometric analysis of affinity purified C3orf1-FL and associated proteins demonstrated that 17 subunits of complex I, and five known assembly factors, copurified with C3orf1-FL (Fig. 5 and Dataset S2); ATP5SL and DNAJC11 were not detected. The most enriched and closely clustered proteins in the analysis were complex I subunits MT-ND1, NDUFA5, NDUFS2, NDUFS3, NDUFS7, and NDUFS8, components of the 315-kDa assembly intermediate (16), plus NDUFA3, NDUFA8, and NDUFA13, components of subcomplex Iα. Therefore, NDUFA3, NDUFA8, and NDUFA13 also are parts of the same assembly intermediate. They were accompanied by assembly factors NDUFAF3 and NDUFAF4, both involved in formation of the 315-kDa assembly intermediate (30). The complex I assembly factors ACAD9, ECSIT, and NDUFAF1 are associated with the 370-kDa assembly intermediate of complex I (31, 32), and have been

CELL BIOLOGY

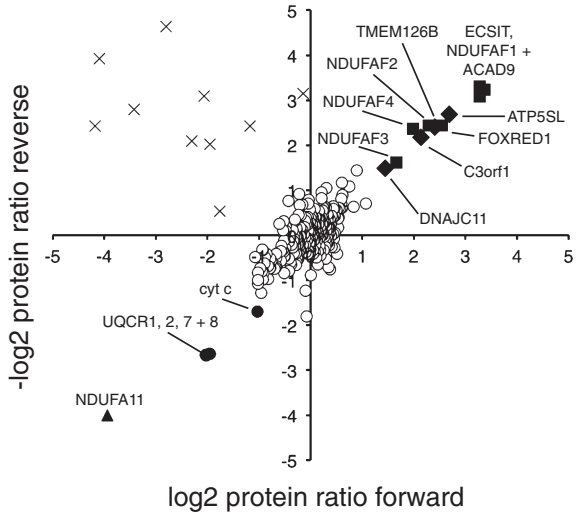

Fig. 3. Exogenous proteins associated with subcomplexes of complex I. Comparison of protein abundance in immunocaptured complex I from control cells and cells with suppressed NDUFA11. Each data point represents a specific protein, and its position corresponds to the abundance ratios from the two complementary heavy and light SILAC experiments. Vertical and horizontal axes represent 1:1 ratios, respectively, where there are no changes in protein abundance between NDUFA11 depleted cells and control cells; ○, proteins with a relative ratio unchanged between the NDUFA11 ablated material and the control; ■, known assembly factors; ◆, enriched proteins with no known role in the assembly of complex I; ▲, complex I subunits that are diminished significantly; ●, proteins diminished by the removal of NDUFA11; X, exogenous contaminants.

reported to comigrate with TMEM126B in native gel profiles (27). Here, isoforms 1 and 5 of TMEM126B were found with relative abundances similar to these extrinsic assembly factor proteins. Mass spectrometric evidence for the isoforms is presented in Fig. S6. There was no evidence for isoforms 2, 3, and 4. Other proteins enriched significantly are constituents of subcomplex Iβ, the distal region of the membrane arm of complex I. The decreasing SILAC protein ratios correspond to membrane protein subunits of increasing distance from the quinone-binding site (Fig. 5). The SILAC ratios of some subunits of complex I were unchanged, indicating that they were not enriched in the complex purified with C3orf1-FL (Dataset S2), and that therefore they are not associated with the 315-kDa subcomplex. They include NDUFA9, which has been reported previously to be a component of the 315-kDa subcomplex (33), although this observation was not corroborated (27). Three other proteins, TMEM126A, HSPA9, and GHITM, also accumulated with C3orf1-FL, but to a much lesser extent than the complex-I–related proteins listed above (Dataset S2).

To demonstrate directly that C3orf1-FL is associated with the 315-kDa subcomplex, the proteins that were immunocaptured with C3orf1-FL were fractionated by blue native (BN)-PAGE, and two protein complexes containing C3orf1-FL were detected by Western blotting, with molecular masses of 315 and 370 kDa, respectively, for the major and minor subcomplexes, respectively (Fig. 5).

Discussion

Supernumerary Subunits and Assembly of Complex I. Sixteen supernumerary subunits are associated with the peripheral arm and 14 are hydrophobic membrane arm components (3). Although their functions are mostly unknown, one subunit, NDUFAB1, is an acyl carrier protein (34); NDUFA9 is related to steroid dehydrogenases (35); NDUFA13 is reported to regulate cell growth and apoptosis (36); and NDUFA2 has a thioredoxin fold (37). As pathological mutations are associated with some supernumerary subunits, those ones probably help to assemble and/or maintain the integrity of the complex. NDUFA11 is an example. It contains two to four predicted transmembrane α-helices

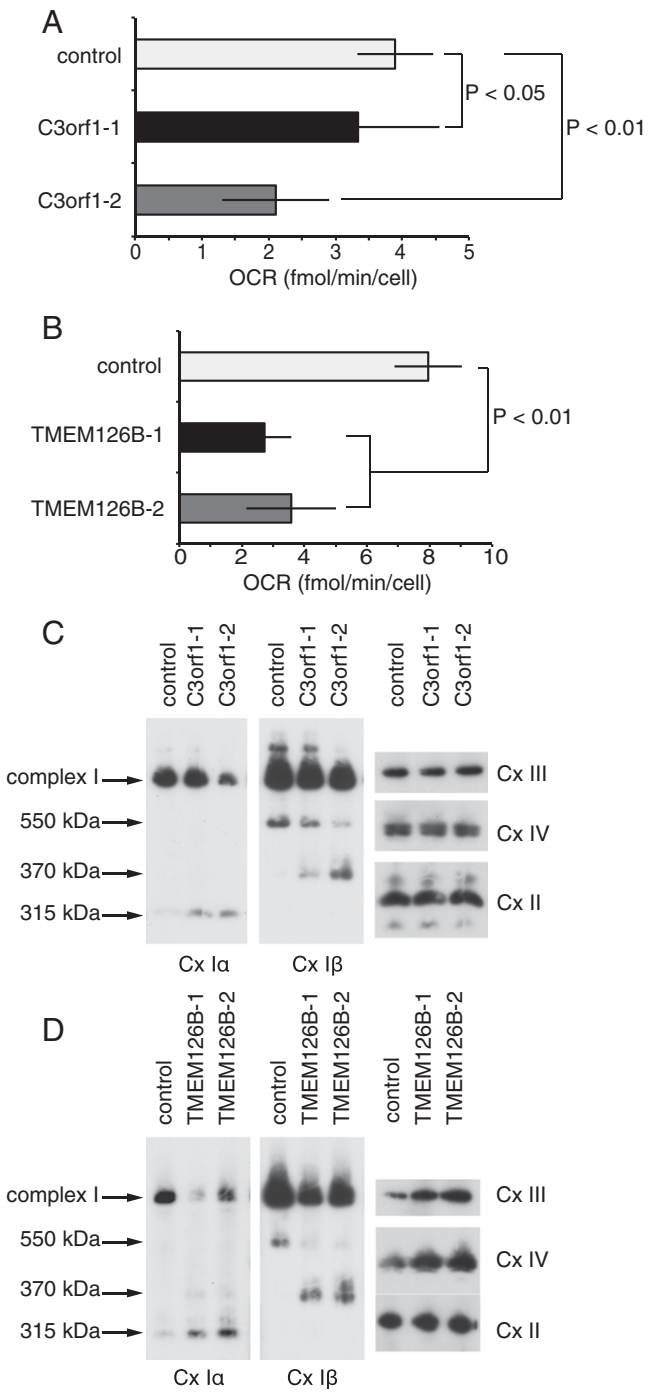

Fig. 4. Ablation of C3orf1 or TMEM126B and the integrity of complex I. The 143B cells were treated with two siRNAs for 96 h, targeted against C3orf1 (50 nM; *A* and *C*) and TMEM126B (100 nM; *B* and *D*). (*A* and *B*) OCR of siRNA-treated 143B cells. The values were corrected by subtraction of a rotenone-treated oxygen consumption value. Error bars represent the SD. (*C* and *D*) Analysis by BN-PAGE of mitoplasts from siRNA-treated 143B cells. The proteins were analyzed by Western blotting with antibodies against the subcomplex Iα subunits NDUFS2 and NDUFA5 in *C* and *D*, respectively, and against the subcomplex Iβ subunit NDUFB8 in both parts. In *C* and *D*, the levels of complexes III, IV, and II are shown on the *Right*.

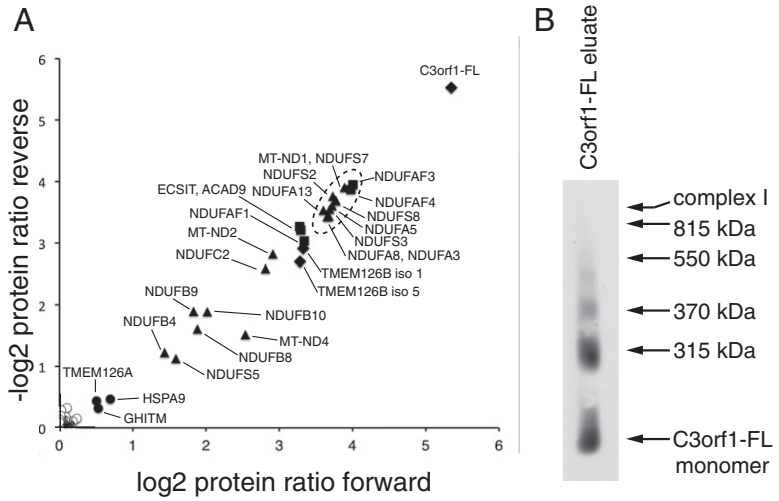

Fig. 5. Proteins interacting with C3orf1. (*A*) The data were obtained by mass spectrometric analysis of material immunocaptured via the FLAG tag in a SILAC experiment conducted with HeLa Flp-In T-Rex cells expressing C3orf1-FL, combined with material from control cells. The upper right quadrant of a scatter plot is shown. It contains the statistically most significant and positively correlated proteins associated with C3orf1-FL. The data points come from forward- and reverse-labeled samples, with the reverse orientation negative. ■, known assembly factors of complex I; ◆, C3orf1-FL and isoforms 1 and 5 of TMEM126B (Fig. S4); ▲, complex I subunits; the encircled cluster contains components of the 315-kDa subcomplex; ●, other proteins with significant SILAC ratios; ○, proteins with an unchanged ratio. (*B*) Proteins associated with C3orf1-FL, fractionated by BN-PAGE, and Western blotted with an anti-FLAG antibody.

and is a component of the membrane region of subcomplex Iα. Human mutations in it result in leukodystrophy (17), and as shown here, it is required for the assembly and/or possibly the structural integrity of complex I. In its absence, subcomplexes of complex I of 550 and 815 kDa accumulate. It has the characteristics of an intrinsic assembly factor.

Extrinsic Assembly Factors. The 37 nuclear-encoded subunits of complex I are imported into the organelle and then sorted, folded, and assembled into the peripheral and membrane arms. The 7 remaining subunits MT-ND1–6 and MT-ND4L are hydrophobic proteins translated from mitochondrial DNA. During sorting, folding, and assembly, they become associated with the 14 other membrane arm subunits encoded in the nucleus. The mitochondrially and nuclear-encoded subunits contribute about 60 and 19 transmembrane α-helices, respectively, to the membrane domain of complex I (6). A further 23 nuclear-encoded subunits are assembled into the peripheral arm of the enzyme, and in the process eight iron–sulfur clusters are incorporated into five core subunits in the extrinsic arm (NDUFS1, NDUFS7, NDUFS8, NDUFV1, and NDUFV2), and a FMN molecule is inserted noncovalently into NDUFV1. This complicated process requires the participation of other proteins not present in the complete complex. Known as extrinsic assembly factors, they are required for producing the complete enzyme. Assembly factors (NDUFAF2–4 and FOXRED1) have been identified via human mutations that impair function (29, 30, 38), by homology with an assembly factor for complex I in *Neurospora crassa* (NDUFAF1) or by copurification with other known assembly factors (ECSIT and ACAD9) (31, 32). The BN-PAGE comigration pattern of TMEM126B with NDUFAF1, ECSIT, and ACAD9 led to its characterization as a complex I assembly factor (27). How these assembly factors function is not known, but they may stabilize the subcomplexes and help to join them to other subcomplexes to build the complete enzyme. Two additional proteins involved in the assembly of complex I, C20orf7 (NDUFAF5) and MidA (NDUFAF7), are predicted to be protein methyltransferases and NDUFAF7 methylates subunit NDUFS2 (39, 40). Ind1 is involved in the assembly of iron–sulfur clusters in complex I and C8orf38 (NDUFAF6) stabilizes subunit MT-ND1 (41, 42).

When the expression of supernumerary subunit NDUFA11 was suppressed, all of the assembly factors found previously in association with subcomplexes of complex I were found, plus C3orf1, ATP5SL, and DNAJC11, but the last two were eliminated as possible assembly factors. C3orf1, and also TMEM126B are targeted to mitochondria, and their influence on the assembly of complex I was confirmed by suppressing their expression. The role of C3orf1 as a complex I assembly factor was supported by the copurification of six known assembly factors with subcomplexes containing C3orf1.

Roles of C3orf1 and TMEM126B. A number of features of C3orf1 and TMEM126B suggest that they may be involved in the assembly of the membrane arm of the complex. First, they are both hydrophobic proteins, predicted to have three and four transmembrane α-helices, respectively. In this respect, they differ from all of the other known extrinsic assembly factors for complex I. However, although they are both mitochondrial proteins, currently direct proof of their presence in the inner membrane is lacking. As NDUFA11 is also a membrane protein, and the complex fails to assemble fully in its absence, it is reasonable to classify it also as a complex I assembly factor probably involved in putting together the membrane arm. Second, C3orf1, and also NDUFA11, are members of the TIM17/22/23 family, related in the region of the second of the transmembrane α-helices of C3orf1 and in the following hydrophilic loop (Fig. S3). TIM17 and TIM23 are mitochondrial inner membrane proteins that form the protein translocation pore, and TIM22 mediates the integration of mitochondrial carrier proteins into the inner membrane of the organelle (43). The association of C3orf1 and NDUFA11 with this group of proteins suggests a possible role for both of them in inserting hydrophobic proteins into the membrane arm of complex I. Third, C3orf1 is found with the 315-kDa subcomplex, where the hydrophobic inner membrane subunit ND1 with eight predicted transmembrane α-helices (35) is a significant component, and TMEM126B is associated with a 370-kDa subcomplex, which contains at least subunits MT-ND2, MT-ND3, MT-ND6, and MT-ND4L (all hydrophobic and containing a total of about 20 transmembrane α-helices).

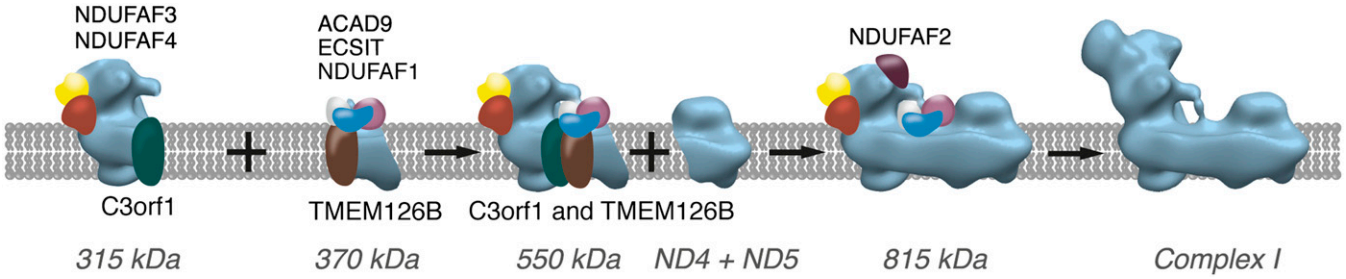

Fig. 6. The pathway of assembly of human complex I. Information from the present and earlier studies has been used (16). The reestimated molecular masses of assembly intermediates (Fig. S2) are used. The image of complex I is from ref. 47.

Assembly Pathway. In current models, the assembly of complex I (15, 16) begins with the formation of a 400-kDa subcomplex (reestimated as 315 kDa), nucleated around core subunits NDUFS2 and NDUFS3, and anchored to the membrane by MT-ND1. The other subunits attributed to this subassembly are NDUFA5, NDUFS7, and NDUFS8. Subunits NDUFA3, NDUFA8, and NDUFA13 can now be added, plus three assembly factors, NDUFAF3, NDUFAF4, and C3orf1. A 460-kDa subcomplex (now 370 kDa) consisting of subunits of the membrane arm of complex I, arises separately, and is likely to contain TMEM126B. In the modified assembly pathway (Fig. 6), the 315- and 370-kDa subassemblies join together to give a subcomplex of 550 kDa (previously 650 kDa). This step was inhibited by the removal of either C3orf1 or TMEM126B, and the 550-kDa subcomplex accumulated in the absence of NDUFA11. Upon addition of the most distal components of the membrane arm, including MT-ND4 and MT-ND5, an 815-kDa (previously 830 kDa) subassembly is formed, lacking only the region of the enzyme that oxidizes NADH. The final step is the addition of the distal region of the peripheral arm (subunits NDUFA12, NDUFS1, NDUFS4, NDUFS6, NDUFV1, NDUFV2, and NDUFV3), aided by the participation of NDUFAF2.

This model of assembly of complex I is incomplete, and the lack of genetic diagnosis of about half the patients with defects in the enzyme (18) suggests that additional extrinsic and/or intrinsic assembly factors remain to be identified.

Methods

Cell Culture. Human 143B osteosarcoma cells (American Type Culture Collection no. CRL8303) and HeLa cells with integrated plasmids pcDNA6/TR and pFRT/lacZeo, constituting the Flp-In T-REx system (Life Technologies) were grown at 37 °C in high (25 mM) glucose medium (DMEM) supplemented with FBS (10% vol/vol), penicillin (100 units/mL), and streptomycin (0.1 mg/mL) under 5% (vol/vol) CO_2. Transfections of DNA and siRNA were performed with Lipofectamine 2000 (Life Technologies).

In SILAC experiments, cells were grown in "heavy" DMEM containing arginine and lysine isotopically labeled with ^{15}N and ^{13}C, and in "light" DMEM containing ^{14}N and ^{12}C arginine and lysine (Sigma-Aldrich). These media were supplemented with proline (200 mg/L) to suppress the conversion of arginine to proline, and with dialyzed FBS (Life Technologies) to prevent dilution of heavy isotopes. To ensure maximal incorporation, the cells were doubled at least seven times in media containing heavy isotopes.

Transcript Suppression. Transcripts were suppressed transiently in duplicate in 143B cells with 30–100 nM siRNA, NDUFA11 with FlexiTube siRNAs (Qiagen), C3orf1 and TMEM126B with Silencer Select siRNAs (Life Technologies), and ATP5SL and DNAJC11 with Mission siRNAs (Sigma Aldrich). Control siRNA (Allstars Negative Control siRNA; Qiagen) was used at the same concentration. Reduction of transcripts was assessed on cDNA (Cells-to-CT kit, Life Technologies) by quantitative real-time PCR (Taqman gene expression assays; Life Technologies). Levels of all target transcripts were reduced by >80% (normalized to β-actin). Where suitable antibodies were available, the reduction in the protein was examined by Western blotting. Four days after transfection, the phenotypes of cells were assessed. Transcripts were suppressed stably in 143B cells by cloning target sequences identical to the siRNA into the pSuperior.puro vector (Oligoengine). Stable recombinants were selected with puromycin (2 μg/mL).

Epitope Tagging and Confocal Microscopy. Human cDNAs encoding C3orf1 (Source BioScience) and TMEM126B (GeneCopoeia) were cloned into pcDNA5/FRT/TO, with sequences for C-terminal FLAG and/or StrepII tags, and incorporated stably into HeLa Flp-In T-Rex cells. Plasmids pOG44 and pcDNA5/FRT/TO containing tagged inserts (1 μg DNA; pOG44:pcDNA5/FRT/TO, 7:1 by weight) were cotransfected. After 24 h, zeocin (50 μg/mL) in the medium was replaced by hygromycin (200 μg/mL). Mitochondria from stable isogenic recombinant clones were labeled with MitoTracker Orange (100 nM; Life Technologies). The cells were fixed with paraformaldehyde (4% wt/vol), permeabilized with Triton X-100 (0.1% vol/vol), and tagged proteins were labeled with mouse M2 anti-FLAG antibody (Sigma-Aldrich) followed by Alexa Fluor 488 goat anti-mouse secondary antibody (Life Technologies). The fluorescence was detected in a Zeiss 510 LSM confocal microscope.

Measurement of Respiration. The oxygen consumption rate (OCR) of 143B cells was measured in an XF24 extracellular flux analyzer (Seahorse Biosciences) as described in ref. 39.

Protein Purification. Expression of proteins in HeLa Flp-In T-Rex cells was induced for 24 h with doxycycline (20 ng/mL). Cells (15 mg protein) were solubilized in PBS with complete EDTA-free protease inhibitor mixture (Roche) and enriched for mitoplasts with digitonin (500 μg/mL; detergent: protein,1:10 wt:wt). Mitoplasts (1.5 mg protein) were solubilized in 1% (wt/vol) n-dodecyl-β-D-maltoside (DDM) in PBS containing protease inhibitor (Roche), glycerol (10% vol/vol), and a mixture of synthetic phospholipids [1-palmitoyl-2-oleoyl-*sn*-glycero-3-phosphocholine, 0.09 mg/mL; 1-palmitoyl-2-oleoyl-*sn*-glycero-3-phosphoethanolamine, 0.03 mg/mL; 1-palmitoyl-2-oleoyl-*sn*-glycero-3-phospho-(1′-*rac*-glycerol), 0.03 mg/mL (Avanti)]. Insoluble material was filtered off. Complex I and subcomplexes were purified at 4 °C with immunocapture resin (Mitosciences), and FLAG-tagged proteins with M2 FLAG agarose (Sigma-Aldrich). Bound proteins were eluted with 0.2 M glycine and DDM (0.05% wt/vol), pH 2.5. Native proteins were eluted in "solubilization buffer," containing 3× FLAG peptide (125 ng/μL) and DDM (0.05% wt/vol).

Electrophoresis and Western Blotting. Protein complexes were fractionated by BN-PAGE in 3–12% acrylamide gradient Bis-Tris gels (Life Technologies). Mitoplasts made with digitonin (2 mg/mL; detergent:protein, 1:2.5, wt:wt), were solubilized in 1.67% (wt/vol) DDM (detergent:protein, 6:1, wt:wt). Fractionated proteins were transferred to a polyvinylidene difluoride membrane and probed with antibodies in PBS with milk powder (approximately 5%, wt:vol) and Tween 20 (0.01%, vol:vol). The antibodies were against complex I subunits NDUFB8 and NDUFA5, subunit 5a of complex IV (CoxVa), the SDHB subunit of complex II, the core 2 subunit of complex III (UQCR2), and β-actin (Sigma-Aldrich). Antibodies against complex I subunits NDUFS1 and NDUFB10 were purchased from Proteintech. A chicken polyclonal anti-peptide antibody was prepared against residues 1–17 of NDUFA11 (Agrisera). The molecular masses of subcomplexes of complex I were estimated from their migration by BN-PAGE. The gels were calibrated with bovine respiratory complexes I and III–V plus standard proteins from a NativeMark kit (Life Technologies).

Mass Spectrometry. Each analysis was based on two SILAC experiments (44), one in which the ablated cells were labeled in heavy medium and the controls in light medium, and the second vice versa. Each sample for mass

spectrometric analysis consisted of a 1:1 mixture of complex I (and its subcomplexes) immunopurified from mitoplasts from control and NDUFA11 ablated cells. They were reduced, alkylated, and fractionated by SDS/PAGE on 10–20% acrylamide gradient gels in Tris-glycine buffer (Life Technologies), and proteins in gel slices were digested with trypsin. Peptides were redissolved in 5% (vol/vol) aqueous acetonitrile containing 0.1% (vol/vol) formic acid. They were fractionated in a Thermo Easy-nLC with a reverse-phase column (75 μm i.d. × 100 mm; Nanoseparations) with a gradient of 0–40% buffer B over 84 min with a flow rate of 300 nL/min (buffers A and B, 5% and 95% aqueous acetonitrile, respectively, each containing 0.1% formic acid). The effluent was passed into an LTQ OrbiTrap XL mass spectrometer (Thermo Fisher) operating in data-dependent MS/MS mode, with a mass scan range of 400–2,000 Da for precursor ions and MS/MS of the top 10 highest abundance ions selected from the full scan. Each tryptic peptide produced a peptide ion pair differing by either 10.01 or 8.01 Da for peptides with C-terminal arginine or lysine, respectively. Peptide pairs were located by MaxQuant and identified with Andromeda by comparison of fragment ion masses in tandem mass spectra and the human UniProt database (45). A heavy:light ratio was calculated with MaxQuant. The median peptide ratio was taken to be the protein ratio, using at least two ratios for each protein. The ratios from each experiment were plotted on horizontal and vertical axes, respectively, of a "scatter plot" as the log base 2 value. Thus, a fourfold change in the abundance of a protein in both experiments becomes 2 on each axis, and the protein is represented by a point in the top right quadrant of the scatter plot. The horizontal and vertical axes represent 2 raised to the power of zero, a ratio of 1, and no changes in abundance. Proteins unaffected by experimental conditions cluster around the origin, and those with consistent increases or decreases in abundance occur in the top right or bottom left quadrants, respectively. A diagonal line from the top right to bottom left represents a perfect correlation between the two experiments. Statistically significant proteins in both orientations of labeling were identified with Perseus (46) ($P < 0.05$). Points in the two other quadrants represent proteins where the differences are irreproducible in the replicate experiments. Those in the top left quadrant contain exogenous contaminants.

ACKNOWLEDGMENTS. This work was supported by the Medical Research Council (MRC). B.A. received an MRC Research Studentship.

1. Baradaran R, Berrisford JM, Minhas GS, Sazanov LA (2013) Crystal structure of the entire respiratory complex I. *Nature* 494(7438):443–448.
2. Walker JE (1992) The NADH:ubiquinone oxidoreductase (complex I) of respiratory chains. *Q Rev Biophys* 25(3):253–324.
3. Carroll J, Fearnley IM, Shannon RJ, Hirst J, Walker JE (2003) Analysis of the subunit composition of complex I from bovine heart mitochondria. *Mol Cell Proteomics* 2(2): 117–126.
4. Balsa E, et al. (2012) NDUFA4 is a subunit of complex IV of the mammalian electron transport chain. *Cell Metab* 16(3):378–386.
5. Chomyn A, et al. (1985) Six unidentified reading frames of human mitochondrial DNA encode components of the respiratory-chain NADH dehydrogenase. *Nature* 314(6012): 592–597.
6. Hirst J, Carroll J, Fearnley IM, Shannon RJ, Walker JE (2003) The nuclear encoded subunits of complex I from bovine heart mitochondria. *Biochim Biophys Acta* 1604(3): 135–150.
7. Sazanov LA, Hinchliffe P (2006) Structure of the hydrophilic domain of respiratory complex I from Thermus thermophilus. *Science* 311(5766):1430–1436.
8. Hirst J (2011) Why does mitochondrial complex I have so many subunits? *Biochem J* 437(2):e1–e3.
9. Efremov RG, Sazanov LA (2011) Respiratory complex I: 'Steam engine' of the cell? *Curr Opin Struct Biol* 21(4):532–540.
10. Finel M, Skehel JM, Albracht SP, Fearnley IM, Walker JE (1992) Resolution of NADH: ubiquinone oxidoreductase from bovine heart mitochondria into two subcomplexes, one of which contains the redox centers of the enzyme. *Biochemistry* 31(46): 11425–11434.
11. Sazanov LA, Peak-Chew SY, Fearnley IM, Walker JE (2000) Resolution of the membrane domain of bovine complex I into subcomplexes: Implications for the structural organization of the enzyme. *Biochemistry* 39(24):7229–7235.
12. Hunte C, Zickermann V, Brandt U (2010) Functional modules and structural basis of conformational coupling in mitochondrial complex I. *Science* 329(5990):448–451.
13. Angerer H, et al. (2011) A scaffold of accessory subunits links the peripheral arm and the distal proton-pumping module of mitochondrial complex I. *Biochem J* 437(2): 279–288.
14. Lazarou M, McKenzie M, Ohtake A, Thorburn DR, Ryan MT (2007) Analysis of the assembly profiles for mitochondrial- and nuclear-DNA-encoded subunits into complex I. *Mol Cell Biol* 27(12):4228–4237.
15. McKenzie M, Ryan MT (2010) Assembly factors of human mitochondrial complex I and their defects in disease. *IUBMB Life* 62(7):497–502.
16. Mimaki M, Wang X, McKenzie M, Thorburn DR, Ryan MT (2012) Understanding mitochondrial complex I assembly in health and disease. *Biochim Biophys Acta* 1817(6): 851–862.
17. Berger I, et al. (2008) Mitochondrial complex I deficiency caused by a deleterious NDUFA11 mutation. *Ann Neurol* 63(3):405–408.
18. Calvo SE, et al. (2012) Molecular diagnosis of infantile mitochondrial disease with targeted next-generation sequencing. *Sci Transl Med* 4(118):118ra10.
19. Fernandez-Moreira D, et al. (2007) X-linked NDUFA1 gene mutations associated with mitochondrial encephalomyopathy. *Ann Neurol* 61(1):73–83.
20. Haack TB, et al. (2012) Mutation screening of 75 candidate genes in 152 complex I deficiency cases identifies pathogenic variants in 16 genes including NDUFB9. *J Med Genet* 49(2):83–89.
21. Hoefs SJ, et al. (2008) NDUFA2 complex I mutation leads to Leigh disease. *Am J Hum Genet* 82(6):1306–1315.
22. Hoefs SJ, et al. (2011) NDUFA10 mutations cause complex I deficiency in a patient with Leigh disease. *Eur J Hum Genet* 19(3):270–274.
23. Kirby DM, et al. (2004) NDUFS6 mutations are a novel cause of lethal neonatal mitochondrial complex I deficiency. *J Clin Invest* 114(6):837–845.
24. Ostergaard E, et al. (2011) Respiratory chain complex I deficiency due to NDUFA12 mutations as a new cause of Leigh syndrome. *J Med Genet* 48(11):737–740.
25. van den Bosch BJ, et al. (2012) Defective NDUFA9 as a novel cause of neonatally fatal complex I disease. *J Med Genet* 49(1):10–15.
26. van den Heuvel L, et al. (1998) Demonstration of a new pathogenic mutation in human complex I deficiency: A 5-bp duplication in the nuclear gene encoding the 18-kD (AQDQ) subunit. *Am J Hum Genet* 62(2):262–268.
27. Heide H, et al. (2012) Complexome profiling identifies TMEM126B as a component of the mitochondrial complex I assembly complex. *Cell Metab* 16(4):538–549.
28. Vogel RO, et al. (2007) Investigation of the complex I assembly chaperones B17.2L and NDUFAF1 in a cohort of CI deficient patients. *Mol Genet Metab* 91(2):176–182.
29. Fassone E, et al. (2010) FOXRED1, encoding an FAD-dependent oxidoreductase complex-I-specific molecular chaperone, is mutated in infantile-onset mitochondrial encephalopathy. *Hum Mol Genet* 19(24):4837–4847.
30. Saada A, et al. (2009) Mutations in NDUFAF3 (C3ORF60), encoding an NDUFAF4 (C6ORF66)-interacting complex I assembly protein, cause fatal neonatal mitochondrial disease. *Am J Hum Genet* 84(6):718–727.
31. Nouws J, et al. (2010) Acyl-CoA dehydrogenase 9 is required for the biogenesis of oxidative phosphorylation complex I. *Cell Metab* 12(3):283–294.
32. Vogel RO, et al. (2007) Cytosolic signaling protein Ecsit also localizes to mitochondria where it interacts with chaperone NDUFAF1 and functions in complex I assembly. *Genes Dev* 21(5):615–624.
33. Ugalde C, et al. (2004) Human mitochondrial complex I assembles through the combination of evolutionary conserved modules: A framework to interpret complex I deficiencies. *Hum Mol Genet* 13(20):2461–2472.
34. Feng D, Witkowski A, Smith S (2009) Down-regulation of mitochondrial acyl carrier protein in mammalian cells compromises protein lipoylation and respiratory complex I and results in cell death. *J Biol Chem* 284(17):11436–11445.
35. Fearnley IM, Walker JE (1992) Conservation of sequences of subunits of mitochondrial complex I and their relationships with other proteins. *Biochim Biophys Acta* 1140(2): 105–134.
36. Zhang J, et al. (2003) The cell death regulator GRIM-19 is an inhibitor of signal transducer and activator of transcription 3. *Proc Natl Acad Sci USA* 100(16):9342–9347.
37. Brockmann C, et al. (2004) The oxidized subunit B8 from human complex I adopts a thioredoxin fold. *Structure* 12(9):1645–1654.
38. Ogilvie I, Kennaway NG, Shoubridge EA (2005) A molecular chaperone for mitochondrial complex I assembly is mutated in a progressive encephalopathy. *J Clin Invest* 115(10):2784–2792.
39. Rhein VF, Carroll J, Ding S, Fearnley IM, Walker JE (2013) NDUFAF7 methylates arginine-85 in the NDUFS2 subunit of human complex I. *J Biol Chem*, M113.518803.
40. Sugiana C, et al. (2008) Mutation of C20orf7 disrupts complex I assembly and causes lethal neonatal mitochondrial disease. *Am J Hum Genet* 83(4):468–478.
41. McKenzie M, et al. (2011) Mutations in the gene encoding C8orf38 block complex I assembly by inhibiting production of the mitochondria-encoded subunit ND1. *J Mol Biol* 414(3):413–426.
42. Sheftel AD, et al. (2009) Human ind1, an iron-sulfur cluster assembly factor for respiratory complex I. *Mol Cell Biol* 29(22):6059–6073.
43. Chacinska A, Koehler CM, Milenkovic D, Lithgow T, Pfanner N (2009) Importing mitochondrial proteins: machineries and mechanisms. *Cell* 138(4):628–644.
44. Ong SE, et al. (2002) Stable isotope labeling by amino acids in cell culture, SILAC, as a simple and accurate approach to expression proteomics. *Mol Cell Proteomics* 1(5): 376–386.
45. Cox J, et al. (2011) Andromeda: A peptide search engine integrated into the MaxQuant environment. *J Proteome Res* 10(4):1794–1805.
46. Cox J, Mann M (2011) Quantitative, high-resolution proteomics for data-driven systems biology. *Annu Rev Biochem* 80:273–299.
47. Clason T, et al. (2010) The structure of eukaryotic and prokaryotic complex I. *J Struct Biol* 169(1):81–88.